

Preprint: Toward Robust and Efficient ML-Based GPU Caching for Modern Inference

Peng Chen¹, Jiaji Zhang¹, Hailiang Zhao^{1*}, Yirong Zhang¹, Jiahong Yu¹, Xueyan Tang², Yixuan Wang³, Hao Li⁴, Jianping Zou⁴, Gang Xiong⁴, Kingsum Chow¹, Shuibing He¹, Shuiguang Deng^{1*}

¹Zhejiang University ²Nanyang Technological University
³Nanjing University of Aeronautics and Astronautics ⁴Kuaishou

Abstract

In modern GPU inference, cache efficiency remains a major bottleneck. In recommendation models, embedding hit rates largely determine throughput, while in large language models, KV-cache misses substantially increase time-to-first-token (TTFT). Heuristic policies such as LRU often struggle under structured access patterns. Learning-based approaches are promising, but in practice face two major limitations: they degrade sharply when predictions are inaccurate, or they gain little even with accurate predictions due to conservative designs. Some also incur high overhead, further limiting practicality.

We present LCR, a practical framework for learning-based GPU caching that delivers performance gains while ensuring robustness and efficiency. Its core algorithm, LARU, enhances LRU with machine-learned predictions and dynamically adapts to prediction accuracy through online error estimation. When predictions are accurate, LARU achieves near-optimal performance. With inaccurate predictions, it degrades gracefully to near-LRU performance. With LCR, we bridge the gap between empirical progress and theoretical advances in learning-based caching.

Experiments show that LCR delivers consistent gains under realistic conditions. In DLRM and LLM scenarios, it improves throughput by up to 24.2% and reduces P99 TTFT by up to 28.3%, outperforming widely used inference systems. Even under poor predictions, its performance remains stable, demonstrating practical robustness.

1 Introduction

In modern GPU inference systems, performance bottlenecks increasingly stem not from computation but from memory access [7, 20, 21, 26, 27, 47]. As deep learning models grow in scale and complexity, from deep learning recommendation models (DLRMs) with terabyte-scale embedding tables [13] to large language models (LLMs) that rely on

extensive key-value (KV) cache reuse [52], the limitations of traditional GPU caching policies become clearly evident. Inefficient caching translates directly into higher latency, reduced throughput, and even degraded service-level agreement (SLA) compliance, particularly under real-world workloads.

The core of this challenge is the scarcity of high-bandwidth memory (HBM) on GPUs. While HBM enables fast data access, its capacity is severely constrained compared to the size of frequently accessed data required by models. Inference workload patterns are typically highly diverse: DLRMs exhibit irregular, sparse embedding lookups, while LLMs generate long sequences with structured KV cache reuse during both prefill and decoding. Conventional eviction policies like LRU rely on simple recency heuristics that fail to capture these access patterns, resulting in frequent cache misses far from the offline optimal [28, 39]. This inefficiency becomes a critical bottleneck, especially when cache misses trigger expensive recomputation or memory transfers.

Cost of blindly trusting ML predictions. To improve cache hit rates, recent systems such as GLIDER [32], LRB [34], and PARROT [22] use machine learning (ML) to predict future accesses and guide eviction decisions. However, these systems often *blindly follow* predictions, with little mechanism to handle mispredictions. This leads to a critical vulnerability: when predictions are inaccurate, which could be caused by, e.g., data drift, cold starts, or adversarial inputs, the cache may evict heavily reused items, causing a cascade of expensive memory accesses. The consequences are severe in GPU inference. In LLMs, a single KV cache miss in SGLang can trigger recomputation of attention states or slow DRAM fetches, drastically increasing time to first token (TTFT) [52]. Because host-to-device access latency differs by orders of magnitude, even a few bad evictions can dominate end-to-end latency. In DLRMs, low embedding hit rates directly reduce throughput and increase average latency [42]. As a result, the risk of *performance collapse under prediction errors* remains a key barrier to deploying ML-based caches in production.

*Corresponding authors: Hailiang Zhao (hliangzhao@zju.edu.cn) and Shuiguang Deng (dengsg@zju.edu.cn).

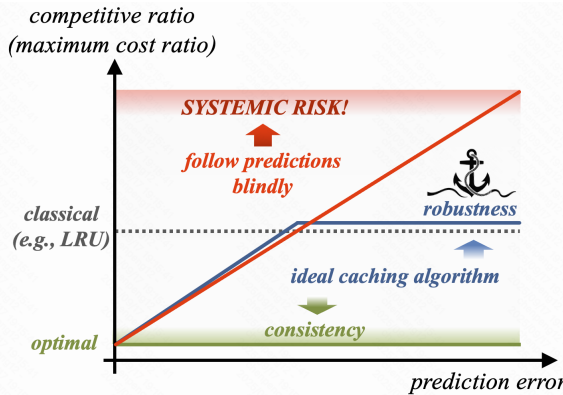


Figure 1: Goals of learning-based caching algorithms.

Promise and Limitations of Caching Algorithms. Motivated by this risk, a line of research called *algorithms with predictions* [24] has emerged.¹ These algorithms aim to achieve two goals: (1) high performance when predictions are accurate, and (2) graceful degradation when predictions are poor. The latter property, termed *robustness*, prevents system-wide performance collapse under poor predictions. Approaches such as PREDICTIVEMARKER [23], BLINDORACLE&LRU [41], and F&R [31] offer elegant theoretical guarantees. However, existing approaches face key limitations: (1) overly conservative use of predictors, limiting gains from accurate predictions; (2) maintaining multiple cache index structures, which incurs prohibitive deployment overhead; and (3) expensive per-request sorting or scanning, leading to high algorithmic cost. As a result, their practical benefits are limited (see Section 2.3). While they demonstrate robustness in theory, their real-world applicability remains constrained.

To rigorously evaluate worst-case behavior, we adopt the *competitive ratio*, i.e., the maximum cost ratio, defined as the number of cache misses incurred by an online algorithm divided by that of the offline optimal algorithm [5].² Unlike average metrics like hit rate, which can obscure tail latency spikes, the competitive ratio provides a worst-case performance bound critical for system stability. In production, even rare cache misses in critical paths can trigger cascading delays and violate SLAs. By bounding the worst-case gap to optimal, this metric ensures *predictable performance* under highly dynamic workloads. Following standard terminology [24], we adopt the term *consistency* to denote the competitive ratio under perfect predictions, and *robustness* to denote the upper bound of the worst-case ratio under arbitrarily inaccurate predictions. As illustrated in Figure 1, our goal is an algorithm

¹See <https://algorithms-with-predictions.github.io/> for a comprehensive collection of the literature.

²A competitive ratio close to 1 indicates near-optimal worst-case performance; the smaller the competitive ratio (closer to 1), the better the algorithm's theoretical guarantee. An algorithm with a competitive ratio of 1 performs as well as the offline optimum even in the worst case. See Technical Appendix A for the formal definition of the competitive ratio.

that approaches near-optimal performance when predictions are good (*consistency*), and degrades gracefully to classical algorithm guarantees when predictions fail (*robustness*).

The limitations of existing approaches, whether vulnerable to errors or too costly to deploy, highlight a critical gap: *Can we design a GPU caching framework that achieves high performance with performance bounds under all prediction conditions, while remaining efficient and practical?*

We answer this with LCR (Learning-based Caching framework with Robustness), a unified framework for learning-based GPU caching. LCR is designed for GPU-based inference workloads with *fixed-size* cache items, such as embedding vectors in DLRMs [42] and KV cache vectors in LLMs [52]. The framework's design generalizes to other scenarios involving reusable GPU-resident data, including ANN search [51] and GNN inference [50]. In this work, we focus on DLRM and LLM deployments to demonstrate its effectiveness. Our contributions are as follows.

- We present LARU, a new learning-based caching algorithm that augments LRU with predictions while dynamically adapting to predictor accuracy. LARU achieves optimal performance when predictions are accurate (*consistency*), and degrades gracefully to LRU-level performance under large errors (*robustness*), with only $O(\log k)$ complexity per request, where k is the cache size.
- We design LCR, a practical framework built on LARU, and integrate it into HugeCTR [40, 42] for DLRMs and SGLang [52] for LLMs. LCR supports different predictors and both synchronous and asynchronous invocation modes, enabling deployment across diverse concurrency levels and latency requirements.
- We evaluate LCR on real workloads with lightweight GBM-based predictors. In DLRM scenarios, it improves SparseLengthsSum (SLS) throughput by up to 24.2% on QB-Video. For LLM serving, it reduces P99 TTFT by up to 10.7% on Aibrix-Synthetic with Qwen2.5-32B, and by 13.5%–28.3% on Online-QA with DeepSeek-R1-671B, while maintaining stable performance even under inaccurate predictions.

The rest of the paper is organized as follows. Section 2 discusses the limitations of existing caching policies and presents our motivation. Section 3 presents LCR, detailing its algorithmic design and system architecture. Sections 4 and 5 evaluate LCR on real-world DLRM and LLM workloads, respectively. Section 6 discusses related work in caching and learning-based algorithms. Finally, Section 7 concludes the paper.

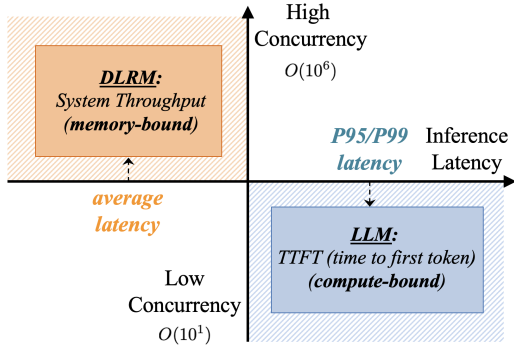


Figure 2: **Key performance metrics differ between DLRMs and LLMs.** (1) DLRMs process requests in tens of milliseconds, enabling high concurrency. System cost is dominated by throughput, making *average latency* the key optimization target. (2) LLMs involve longer sequences and heavier computation, resulting in lower concurrency. User experience depends heavily on *tail latency*, particularly P95/P99 TTFT, which is strongly influenced by KV cache hit rates.

2 Background and motivation

2.1 GPU caching in production systems

In this paper, we focus on two representative model inference scenarios, DLRMs and LLMs, where effective GPU caching is critical for performance. As shown in Figure 2, these scenarios exhibit distinct characteristics: DLRMs typically run at high concurrency, where throughput is the primary metric, whereas LLMs operate at lower concurrency and are highly sensitive to tail latency, particularly P95 or P99 TTFT mandated by SLAs. Despite these differences, both benefit substantially from higher hit rates in GPU-resident data. Figure 3 illustrates the GPU cache data flow in both inference pipelines.

DLRMs. Deep learning recommendation models (DLRMs) rely on massive embedding tables, often hundreds of gigabytes in size, to convert sparse categorical inputs into dense vectors. Due to limited GPU HBM capacity, only a small and frequently accessed subset can be cached on-device; the rest reside in CPU memory or remote storage. Access patterns are typically irregular and sparse, breaking memory locality and limiting data reuse. Under high concurrency, this leads to poor effective memory bandwidth from DRAM, making DLRM workloads strongly *memory-bound*. Cache misses incur high latency, and system throughput is highly sensitive to embedding hit rates. This bottleneck is well documented in both academic [6, 17, 19, 21] and industrial [8, 13, 14, 16, 53] studies. Alibaba, for instance, reported that over 60% of inference latency in production systems stems from embedding lookups [13, 14], highlighting the importance of embedding caching. To address this, frameworks like HugeCTR [40, 42] introduce GPU-side embedding caching with LRU-based

eviction, achieving up to $2.35\times$ throughput improvement over TensorFlow baselines at batch size 2048. UGache [33] improves further with a unified multi-GPU caching architecture, hotness-aware metrics, and factored extraction, achieving up to $5.25\times$ training speedup in GNNs and $3.45\times$ in recommendation inference. However, like other heuristic approaches, UGache lacks efficient predictive caching strategies.

LLMs. During inference, the prefill phase processes n prompt tokens through self-attention, incurring $O(n^2)$ compute cost per request without KV cache reuse. Without caching, each request recomputes the full attention context from scratch, making the workload strongly *compute-bound*, especially for long prompts, and increasing TTFT significantly. KV cache reuse avoids redundant computation: by storing and reusing key-value states from prior inferences, shared prefix sequences need not be recomputed. Full reuse reduces cost to $O(n)$, drastically lowering TTFT. This is crucial for tail latency, as P99 delays are often driven by long-context requests such as multi-turn conversations, where prior turns are appended as prefixes to maintain *contextual memory*. Real-world workloads like ShareGPT [1] show that 73% of requests involve multi-turn interactions or structured prompts, exhibiting strong inter-request prefix similarity. This creates significant opportunities for cross-request KV cache sharing. Modern frameworks such as vLLM [18] and SGLang [52] exploit this using RadixTree to manage shared prefixes efficiently, achieving up to $6.4\times$ throughput improvement. However, KV caching demands careful memory management: a single 2K-token request in an OPT-30B-sized model consumes about 2.6GB of KV cache, while model weights require over 50GB of GPU HBM. This results in tight memory budgets and places high demands on cache replacement efficiency [52]. Despite these constraints, recent studies [39] show that KV reuse, though skewed, exhibits strong temporal predictability.

Frameworks such as HugeCTR [42] and Fleche [43] for DLRMs, and vLLM [18] and SGLang [52] for LLMs, universally adopt LRU as their default eviction policy. While simple and efficient, LRU assumes recency predicts reuse, which often fails under dynamic, non-stationary, or scan-heavy access patterns [29]. To quantify this, Figure 4 reports embedding cache hit rates for DLRMs (AD-CTR-User and QB-video, batch size 128) and KV-cache hit rates for LLMs (Online-QA and Aibrix-Synthetic). The gap between LRU and the offline optimal (OPT) ranges from 15.6% to 23.6% for DLRMs, and reaches 28.7% on Online-QA and 23.3% on Aibrix-Synthetic for LLMs. Given the high cost of a miss, even small hit rate gains yield large system benefits: increasing hit rate from 50% to 55% reduces misses by 10%, leading to nearly a 10% throughput gain in production.

With diverse models and deployments, static heuristics fall short. This yields our first insight:

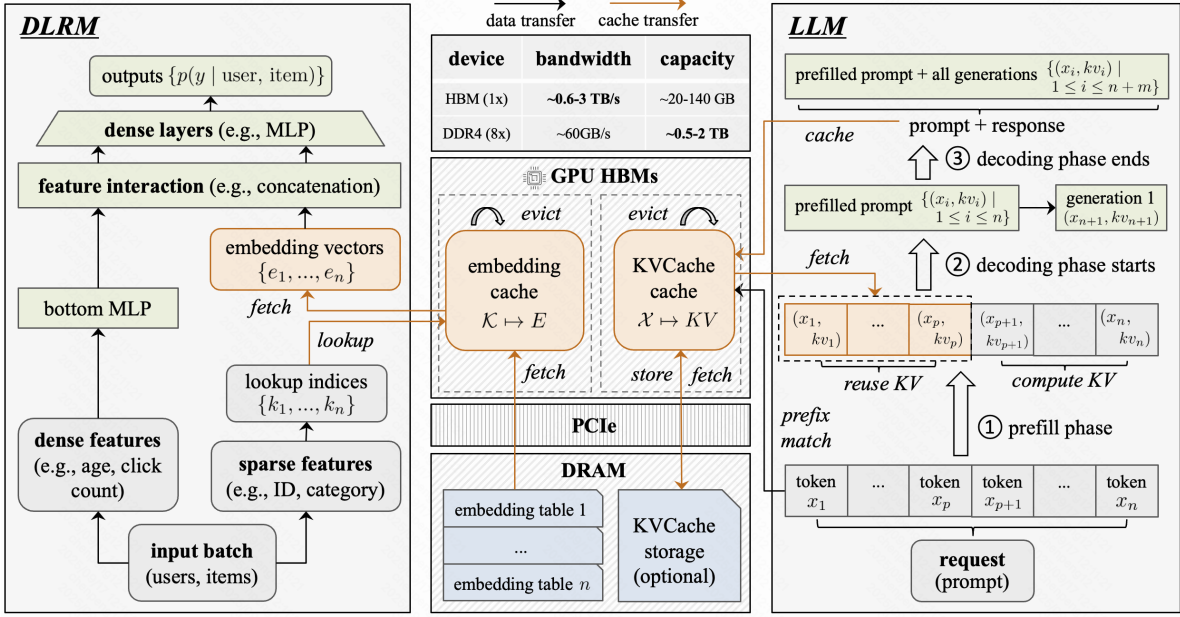


Figure 3: **Illustration of two GPU caching use cases.** (1) **DLRMs**: Inputs contain dense features and sparse features (e.g., user ID, product category). Dense features are processed by a bottom MLP, while sparse features are mapped into embedding vectors via large pre-trained tables, often stored hierarchically in GPU HBM and DRAM. (2) **LLMs**: Each request prompt is a token sequence whose KV vectors are computed during the prefill phase. If KV vectors for a prefix are cached in GPU HBM, they are reused. During decoding, the KV matrices for both the prompt and the generated tokens are cached in GPU HBM.

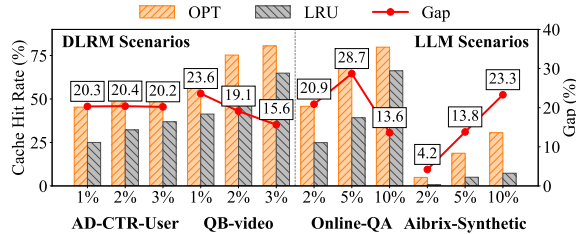


Figure 4: Cache hit rate gap between LRU and the offline optimum (OPT) under varying cache ratios.

Conventional cache replacement policies struggle under dynamic inference workloads, motivating the use of ML to adapt to evolving access patterns.

2.2 Existing learning-based caching systems

To address the limitations of heuristic policies, recent work has explored learning-based caching [12, 22, 29, 32, 34, 35, 38, 44, 45, 46, 54], summarized in Table 1. These systems use learned predictions to guide eviction decisions. For example, GLIDER [32] uses an SVM to classify items as cache-friendly or cache-averse, evicting the latter. LRB [34] first uses gradient boosting machines (GBM) to predict the next-request time and then generates a similar binary classification based

on a threshold. 3L-CACHE [54] improves sampling with bi-directional traces but still blindly follows GBM-predicted next-request times. Reinforcement learning approaches [35, 45] also directly act on prediction outputs. We classify such strategies as FPB (*Follow Prediction Blindly*): a naive policy that evicts the item with the highest predicted priority, such as the farthest next-request time. The core flaw of FPB is its lack of robustness: performance degrades sharply under prediction errors, with no theoretical guarantee on worst-case behavior. More conservative designs, such as HALP [35] and MAT [45], adopt a hybrid approach: they use LRU to pre-select a small set of eviction candidates, then apply ML to score and rank them. We denote this class as HF (*Heuristic-Filtered*). While HF improves empirical stability by limiting ML's influence, it sacrifices potential gains. When predictions are accurate, the heuristic filter may exclude high-value items, capping performance below what ML could achieve.

Figure 5 illustrates these limitations using the *bzip* trace from the public benchmark of the 2nd Cache Replacement Championship (CRC 2017) [2]. The cost ratio, which is defined as algorithm misses divided by OPT misses, is shown across noise levels. At zero noise, all predictions are correct; at noise probability p , each prediction has a chance p of being flipped (e.g., next-request time negated or binary label inverted). At $p = 1$, predictions are fully adversarial. We compare classical heuristics (LRU, MARKER [9], modern designs (LHD [4], SIEVE [49]), and learning-based approaches. FPB

Table 1: Existing representative learning-based caching systems. We abbreviate *Follow Prediction Blindly* as FPB and *Heuristic-Filtered* as HF. The prediction column denotes the value learned by the ML model. *Binary priority* indicates whether the offline optimal would evict the item next (1 if yes, 0 otherwise). *Next-request time* specifies when the item will be reused. *Decision* refers to the optimal eviction action.

Algorithm	ML Model	Prediction	Classification
GLIDER [32]	SVM	binary priority	FPB
LRB [34]	GBM	next-request time	FPB
3L-CACHE [54]	GBM	next-request time	FPB
RAVEN [11]	Mixture Density Network	next-request time	FPB
PARROT [22]	LSTM + attention	decision	FPB
LECAR [38]	Reinforcement Learning	decision	FPB
CACHEUS [29]	Reinforcement Learning	decision	FPB
HALP [35]	1-hidden layer MLP	binary priority	HF
MAT [45]	GBM	next-request time	HF

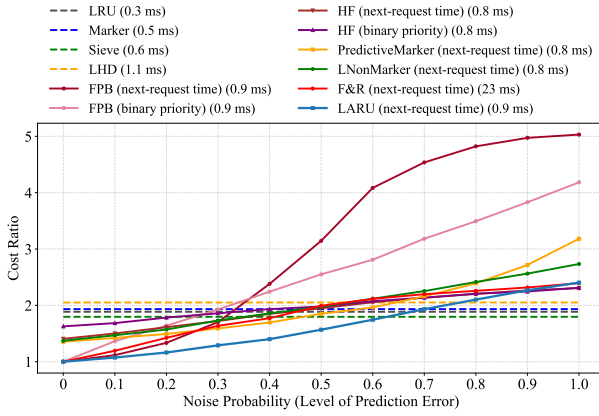


Figure 5: Cost of caching algorithms with different types of predictions, measured relative to the offline optimal. A value of 1 indicates performance equal to the offline optimal.

and HF represent typical algorithms used in systems in Table 1. Since systems such as PARROT [22], which directly predict optimal decisions, are highly error-prone, we only compare next-request time and binary priority predictions in Figure 5. Other learning-based algorithms are included but discussed later (Section 2.3). As shown, HF fails to capitalize on accurate predictions, often performing no better than LHD. In contrast, FPB achieves strong gains at low noise but collapses under prediction errors, sometimes performing worse than LRU. This vulnerability is confirmed in our evaluations across DLRMs and LLMs (see Sections 4 and 5). Such unreliability is a major barrier to deployment in production systems. This leads to our second insight:

To enable safe deployment of learning-based caching, policies must provide bounded robustness guarantees, ensuring graceful degradation without catastrophic failure, even under severe prediction errors.

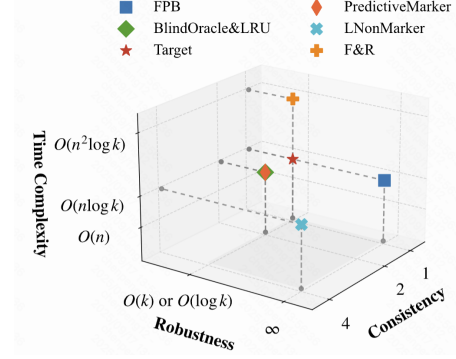


Figure 6: Comparison of performance guarantees among representative learning-based caching algorithms.

2.3 Theoretical algorithms and their limits

Recent theoretical work has advanced learning-based caching with robustness guarantees [25], yet a gap remains between theory and practice. These algorithms are evaluated on *consistency* (performance under perfect predictions) and *robustness* (worst-case performance under large errors). But real-world systems demand a third dimension: *efficiency*, which measures runtime overhead and implementation complexity.

As shown in Figure 6, FPB achieves ideal 1-consistency by evicting the item with the farthest predicted next request, matching the offline optimum when predictions are accurate. However, it has no bounded robustness: a single bad prediction can trigger an unbounded competitive ratio. BLINDORACLE&LRU [41] improves robustness to $2k$ by switching to LRU under poor predictions, but its consistency is 2, limiting hit rate even under perfect predictions. Note that k is the cache size. In addition, it requires maintaining multiple parallel caches. This is prohibitive in GPU systems where metadata access and synchronization are expensive, especially with hierarchical structures like RadixTree in SGLang [52]. Other algorithms face different trade-offs. PREDICTIVEMARKER [23] achieves $4H_k$ -robustness by augmenting MARKER [9], but its consistency is also capped at 2 (see Figure 5). Here $H_k = \sum_{i=1}^k \frac{1}{i} \in [\ln(k+1), \ln k + 1]$. LNON-MARKER [30] lacks robustness bounds. F&R [31] achieves ideal 1-consistency and $O(\log k)$ -robustness, but its amortized $O(n \log k)$ per-request complexity is infeasible for real-time systems. Here n is the total number of page requests. In contrast, practical algorithms achieve $O(\log k)$ per-access cost by maintaining a priority queue over cached items. The legend of Figure 5 empirically demonstrates that the average algorithmic time cost (excluding predictor invocations) of F&R is high at 23 ms, more than 20 \times that of any other algorithm when processing about 2×10^4 requests from the bzip trace.

Figure 6 also highlights our target: an algorithm with 1-consistency, good robustness ($O(k)$ or $O(\log k)$), and system efficiency ($O(\log k)$ per request). We show in Section 3.4 that LARU achieves this. Its empirical performance is validated

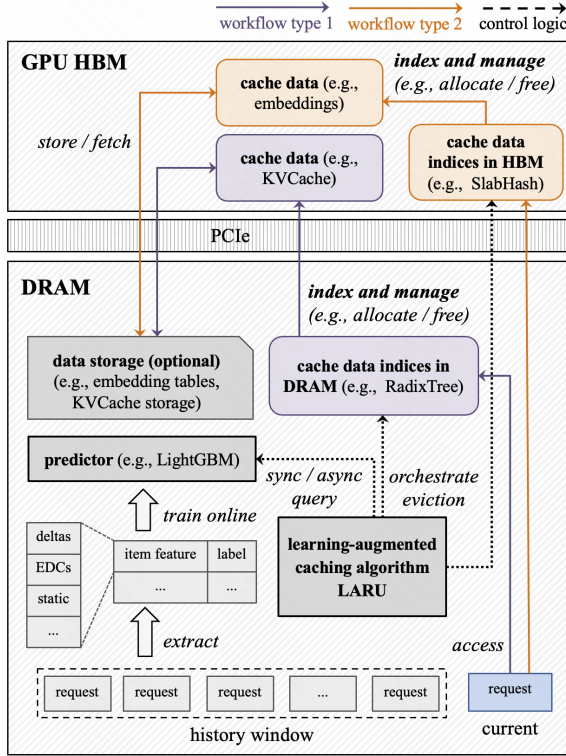


Figure 7: LCR’s architecture and workflows.

in Figure 5 and Sections 4-5. In summary, existing algorithms suffer from: (1) suboptimal consistency, (2) lack of robustness, or (3) prohibitive overhead. This leads to our insight:

A high-performance caching system requires an algorithm that achieves near-ideal consistency, provable robustness, and practical efficiency.

3 LCR

3.1 System design overview

We present LCR, a GPU caching system that closes the gap between theoretical learning-based algorithms and practical efficiency. Its design centers on three components: a lightweight online *predictor*, the LARU caching algorithm, and flexible *index structures* for HBM and DRAM. Together, they enable high hit rates under accurate predictions, robustness to noise, and low metadata overhead, achieving the efficiency-consistency-robustness target outlined in Section 2.3.

Figure 7 presents the architecture of LCR. It operates as follows: incoming requests are tracked in a sliding history window, from which features and labels (e.g., next-request time) are extracted to train the predictor *online*. At cache access or eviction time, LARU queries the predictor, either *synchronously* (blocking) or *asynchronously* (non-blocking),

to obtain eviction priorities. These priorities are then applied by the cache indices, which manage data in HBM (e.g., embeddings, KV cache) with optional DRAM backing. LCR supports two deployment workflows to optimize for latency and resource usage:

- **Workflow 1 (purple):** Indices are stored in DRAM to manage data in HBM, suitable for low-concurrency scenarios such as LLMs.
- **Workflow 2 (orange):** Indices are stored in HBM to manage cache data, suitable for high-concurrency scenarios that require warp-level GPU operations, such as DLRMs.

3.2 LightGBM as the predictor

The predictor in LCR must satisfy strict system requirements: it must deliver accurate predictions in microseconds, incur minimal memory overhead, and adapt quickly to evolving workloads, without contending with GPU compute or HBM used by the model itself. Prior learning-based systems fail under these constraints. Deep models (e.g., Raven [11], Parrot [22]) incur millisecond-scale inference latency and consume significant HBM, directly competing with KV cache and embeddings. Reinforcement learning approaches (e.g., LeCaR [38], CACHEUS [29]) suffer from slow adaptation and high inference cost, making them unsuitable for dynamic LLM workloads.

We adopt LightGBM [15] as our predictor, a gradient-boosted decision tree model that strikes the right balance between accuracy and efficiency. It supports fast online training (sub-100ms for tens of thousands of samples), microsecond inference latency, and low memory footprint (a few percent of cache capacity). Crucially, it runs on CPU, avoiding GPU HBM and compute contention. We use lightweight, interpretable features: (1) *Request intervals (deltas)*: capture recency and periodicity; (2) *Exponentially decayed counters (EDCs)*: track frequency with temporal weighting; (3) *Static metadata*: e.g., tensor type, layer ID, for object identity. These features enable accurate next-access time prediction while remaining computationally and memory-efficient. Furthermore, LCR integrates prediction into LARU’s eviction logic in both synchronous and asynchronous modes, ensuring that predictions improve caching without becoming a bottleneck.

3.3 Cache data indices

LCR is designed as a *unified* caching framework: its learning-based eviction logic (LARU) and predictor interface are decoupled from the underlying data structure. At the same time, LCR exploits the structural properties of cache indices to accelerate prediction-driven eviction and minimize overhead. We instantiate two representative designs in evaluation (Sections 4-5).

SlabHash. We adopt SlabHash [3], a GPU-optimized hash table adapted from HugeCTR for DLRM-style workloads. It organizes memory into fixed-size slots grouped into *slabs* and *slabsets*, enabling *warp-synchronous probing* and batched updates. This design maximizes memory coalescing and minimizes bank conflicts, achieving high throughput under skewed access patterns. Crucially, SlabHash’s flat, array-like layout allows LCR to efficiently maintain and update eviction priorities (e.g., predicted next-access time) as metadata within slabs. The uniform access cost across entries ensures that LARU’s eviction decisions do not introduce variable latency, preserving the predictability required for real-time inference.

RadixTree. We integrate RadixTree [52] for LLM serving, a prefix-aware tree structure that naturally captures reuse across request generations. Each node represents a token in the sequence, and paths correspond to KV cache prefixes. This enables efficient *shared caching* of partial sequence prefixes, reducing memory footprint. LCR leverages the tree’s hierarchical structure to propagate and aggregate prediction signals. For example, frequently reused prefixes can typically be assigned higher persistence scores, while leaf nodes are evicted more aggressively.

While LCR supports both designs through a common interface, which abstracts away insertion, lookup, and eviction primitives, it remains aware of index semantics.

3.4 The LARU algorithm

As discussed in Section 2, blindly trusting predictions can lead to catastrophic cache thrashing under errors. A practical algorithm should exploit accurate predictions to reduce misses and detect and react to prediction errors in real time. We present LARU (Learning-Augmented LRU), a deterministic caching algorithm that achieves both goals through a lightweight, system-friendly design. LARU enhances LRU with prediction-driven evictions, safeguarded by real-time prediction error detection and adaptive prediction confidence.

Misprediction as detectable event. LARU is built on a simple but powerful observation: in the offline optimal algorithm OPT that follows Belady’s rule, an item is never kept in the cache if it is not requested between its eviction and the next request of another item; otherwise, the policy is suboptimal (see Technical Appendix B for a formal description). Hence, upon a cache miss for item x , if there exists an item in the cache that has remained unrequested since the last prediction-driven eviction of x , this indicates prediction errors in that eviction. We refer to this type of cache miss as a *prediction-induced miss*, which is directly observable at runtime without offline analysis.

Unlike measuring the error between predicted and true next-request times, which only indirectly reflects cache per-

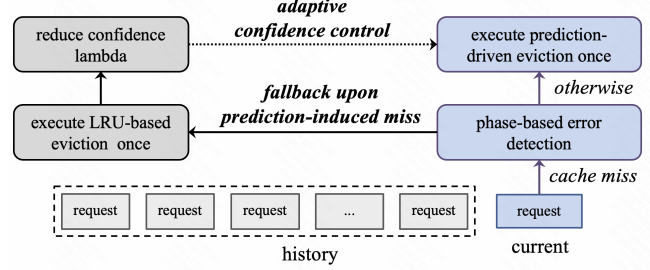


Figure 8: LARU’s algorithmic process on a cache miss.

formance, detecting prediction-induced misses is more meaningful, as it both reveals prediction errors and shows their direct impact on cache behavior. Moreover, detecting such misses prevents continuous cache misses from a single misprediction. For example, in FPB, if a frequently accessed item is repeatedly evicted due to overestimated reuse intervals, the system suffers continuous misses, which can severely degrade throughput in latency-sensitive applications and even cause systemic risk.

Thus, detecting prediction-induced misses early is crucial, as it enables the system to mitigate damage by reverting to a safe policy and reducing subsequent reliance on predictions. This insight motivates the core mechanisms of LARU: *phase-based error detection*, which tracks prediction-driven evictions, and *adaptive confidence control*, which dynamically controls the use of predictions.

Algorithm overview. LARU (Algorithm 1) organizes execution into *phases*. At the start of each phase, all cached items are marked as *old*, and a new phase begins when every old item has been evicted or accessed at least once. When a cache miss occurs, LARU checks whether the requested item was evicted earlier based on predictions (Line 25) in the current phase. If so, this is treated as a prediction error: the algorithm performs one eviction using the LRU policy as a safe fallback and decreases the prediction-confidence parameter λ , which determines the candidate set size for future prediction-driven evictions. This design is inspired by heuristic filtering (HF), but unlike HALP [35], which fixes the candidate set size at 4, LARU adjusts it dynamically, thereby avoiding both overly conservative and overly aggressive use of predictions. If no such error is detected, LARU restricts its eviction choice to the top- l candidates in the LRU queue, where $l = \max(\lfloor \lambda k \rfloor, 1)$. Among these, it evicts the item with the largest predicted next-request time (Line 25). Predictions are updated either synchronously when needed (**SYNC** mode) or asynchronously under specific conditions (**ASYNC** mode), allowing flexibility in system integration.

LARU’s key advantages are both empirical and provable. Theoretically, LARU achieves the target shown in Figure 6:

Algorithm 1 LARU

```
1: Initialize unrequested old items:  $O \leftarrow \emptyset$ 
2: Initialize prediction table  $\mathcal{P} \leftarrow \emptyset$ 
3: Select  $b$  such that  $\log_b(k) \leq k$  (e.g.,  $b = 2$ )
4: Set mode  $\in \{\text{SYNC, ASYNC}\}$ 
5: while a request for item  $x$  arrives do
6:   if  $x$  is already in the cache then
7:      $O \leftarrow O \setminus \{x\}$ 
8:   else if the cache is full then
9:     if  $O = \emptyset$  then
10:      Start a new phase
11:       $O \leftarrow \{\text{all pages currently in the cache}\}$ 
12:       $\lambda \leftarrow 1$ 
13:    end if
14:    if  $x$  was evicted by predictions (Line 25) earlier in
       this phase then
15:      Evict an item  $z$  according to LRU policy
16:       $\lambda \leftarrow \lambda/b$ 
17:    else
18:       $\mathcal{L} \leftarrow \text{top-}l \text{ items that LRU would select for evi-}
         \text{ction, where } l = \max(\lfloor \lambda k \rfloor, 1)$ 
19:      if  $l = 1$  then
20:        Evict the single item  $z \in \mathcal{L}$ 
21:      else
22:        if mode = SYNC then
23:          Predict the reuse interval for each  $y \in \mathcal{L}$  and
             update  $\mathcal{P}(y)$ 
24:        end if
25:        Evict the item  $z \in \mathcal{L}$  with the largest predicted
             next-request time based on  $\mathcal{P}$ 
26:      end if
27:    end if
28:     $O \leftarrow O \setminus \{z\}$ 
29:    Load item  $x$  into the cache
30:  end if
31:  if mode = ASYNC and conditions are satisfied then
32:    Asynchronously predict for item  $x$  and update  $\mathcal{P}(x)$ 
33:  end if
34: end while
```

it ensures a safe fallback to near-LRU performance under prediction errors ($O(k)$ robustness), achieves optimal hit rates under perfect predictions (1-consistency), and incurs an amortized time complexity of $O(\log k)$ per request. See Technical Appendix C-E for detailed proofs. LARU remains efficient even under high-throughput GPU caching workloads, as k is typically small in practice (e.g., 64 in embedding buckets [3] and usually fewer than 10^4 in paged KV caches [18, 52]). Furthermore, LARU reduces predictor invocations. In ASYNC mode, updates are triggered sparingly, while in SYNC mode, a prediction-induced miss results in an LRU-based eviction, suppressing one prediction-driven eviction. Moreover, when λ is small enough that the candidate set size L is one, prediction

invocations are skipped.

4 Evaluation in DLRM Scenarios

4.1 Implementation

SLS operation benchmark. To isolate the impact of caching, we develop a dedicated benchmark integrated with LCR that decouples the SparseLengthsSum (SLS) operation from the HugeCTR framework [42], using Redis as a DRAM-based backend. The SLS operation is a core primitive in DLRMs, and production-scale studies [16] show it dominates inference latency at realistic batch sizes, accounting for 73.5% of total runtime in RMC2-small and 68.9% in RMC2-large. The operation follows a *gather-reduce* pattern, $Output = SLS(Emb, Indices, Lengths)$, where the embedding table Emb is an [Emb size, vector size] matrix, Indices is a vector of sparse IDs specifying which embeddings to retrieve, and Lengths records the number of indices per sample. For each sample, the operation gathers the embedding vectors referenced by Indices and reduces them into a pooled output vector of dimension [batch size, vector size].

Following common industry practice, each embedding vector is configured with 128 floats, occupying 512 bytes. Consistent with prior work [16], we set the SLS pooling size to 50, so that each sample aggregates approximately 50 embedding entries, matching representative DLRM benchmarks. In our experiments, the full embedding tables are stored in DRAM, while only a portion is cached in GPU HBM. The cache index follows the SlabHash structure in HugeCTR [3], stored in GPU HBM. Each slabset consists of two slabs, and each slab contains 32 slots, enabling efficient warp-level operations. Each item (embedding vector) is hashed to a unique slabset, and the caching algorithm operates locally within that slabset.

LARU and baselines settings. Given that each slabset in SlabHash has a capacity of $32 \times 2 = 64$ slots, the parameter b in LARU is set to 2, striking a balance between excessive sensitivity and insensitivity to prediction error. For each slabset, LARU uses a hash table to record prediction-driven evictions, implemented as a lightweight 8192-bit bitset. The total size of these hash tables accounts for only about 3% of the cache size (corresponding to 0.03% of the total size under a 1% cache ratio), which is sufficiently small. We include LRU as a heuristic baseline due to its widespread adoption in current DLRM inference frameworks. FPB (*Follow Prediction Blindly*) serves as a learning-based baseline, representing typical algorithms used in systems such as LRB [34], 3LCACHE [54], and RAVEN [11]. HF is another baseline that implements a heuristic-filtered strategy, adopted by HALP [35] and MAT [45]. For fairness, all learning-based algorithms use the same LightGBM predictor.

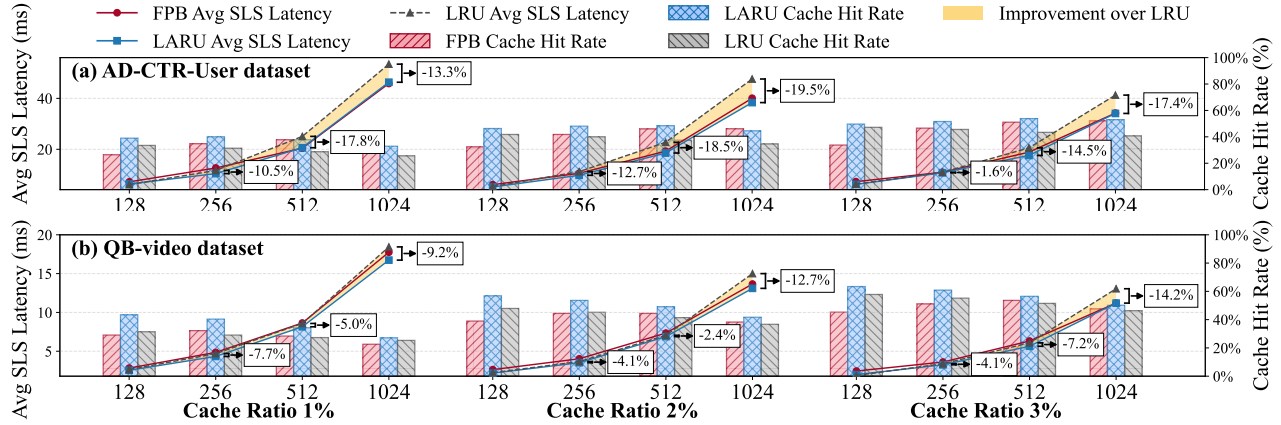


Figure 9: **Average SLS latency improvement across different cache ratios and batch sizes.** FPB and LARU employ the same LightGBM predictor. Numbers in boxes denote LARU’s improvement over LRU. Results are reported for (a) AD-CTR-User and (b) QB-video datasets, evaluated at cache ratios of 1%, 2%, and 3%. The cache ratio is cache size over total distinct items.

Predictor settings. Due to the high concurrency of DLRM workloads, LightGBM is queried and executed in *asynchronous mode* for all learning-based algorithms, ensuring it is offloaded from the critical inference path. A background prediction task is triggered upon the arrival of requests, but only if the previous task has completed, which can prevent task accumulation. For a batch of requests, we check each item and perform prediction only for those that satisfy this condition. This setup corresponds to Workflow type 2 in Figure 7. LightGBM inference is highly efficient: it completes a batch of 2.5×10^4 predictions in under 2ms. Notably, a query with an SLS batch size of 512 contains approximately 2.5×10^4 keys before deduplication. Thus, the latency of this background inference task is much smaller than the total inference latency at batch size 512, where the SLS operation alone takes at least 6ms (see Figure 9). For efficiency, LightGBM uses only four features to predict next-request times: the current timestamp, the item key, the request count, and the most recent request interval.

Hardware settings. Experiments are conducted on a bare-metal server equipped with two NVIDIA A10 GPUs and 512GB of DDR4 DRAM. The GPUs provide a memory bandwidth of approximately 600GB/s, while the DRAM offers about 60GB/s for random reads.

4.2 Datasets

We evaluate on two real-world Click-Through Rate (CTR) datasets: one collected from the production environment of a leading global short-video platform (anonymized as Company A for confidentiality), and the other derived from the public Tenrec benchmark [48] released by Tencent, a major global social networking company.

1. **AD-CTR-User:** This is collected from online user ID embedding queries in advertisement recommendation, deployed in Company A’s production DLRMs. It focuses on user ID lookups, providing a simple yet representative dataset for evaluating CTR performance. The total number of embedding vectors is consistent with large-scale industrial deployments.
2. **QB-video:** This is a subset of the Tenrec benchmark [48] built from large-scale user interactions on Tencent’s video recommendation platforms. It includes millions of user–item interactions with positive feedback (e.g., clicks, likes, shares, follows) and implicit negatives, as well as auxiliary information such as content categories and temporal signals, enabling realistic CTR evaluation.

4.3 Experimental results

The key to improving SLS throughput lies in reducing the average latency of SLS operations. To this end, we evaluate SLS performance using the *average latency* metric, consistent with HugeCTR [42].

Figure 9 presents results on the AD-CTR-User and QB-video datasets, comparing average SLS latency under different caching policies across varying cache ratios and batch sizes. Given that the total size of embedding tables in real-world deployments often exceeds 1 TB, we restrict cache ratios to at most 3%. Across both datasets, LARU consistently reduces SLS latency while achieving higher cache hit rates. On AD-CTR-User, LARU reduces average latency by up to 19.5%, with the largest gains observed at high batch sizes. Similar improvements are seen on QB-video, with latency reductions of up to 14.2%, corresponding to 24.2% and 16.6% higher SLS throughput, respectively. These gains increase with batch size, as larger batches amplify concurrency and the frequency of DRAM random accesses. Overall, LARU substantially

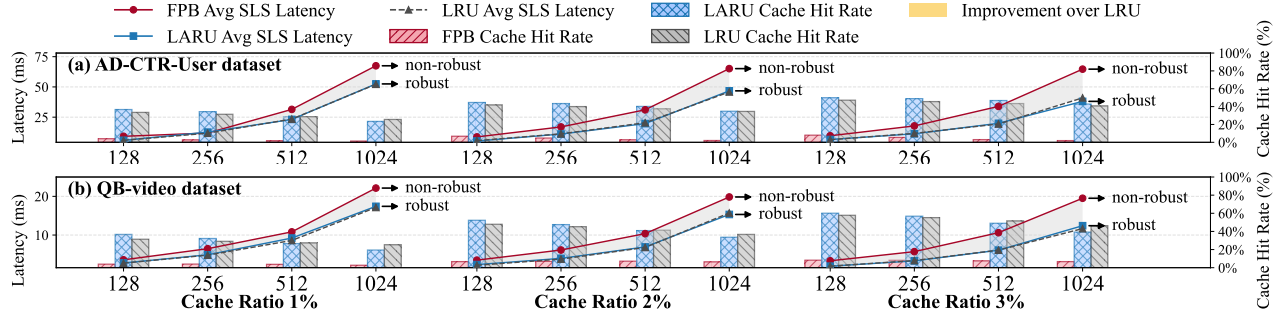


Figure 10: **Robustness Verification.** Average SLS latency under different batch sizes and cache ratios (1%-3%) on (a) AD-CTR-User and (b) QB-video datasets. Both FPB and LARU use the same low-accuracy LightGBM predictor to assess robustness.

improves SLS throughput, particularly at the large batch sizes common in production environments.

Robustness Verification. We empirically verify the robustness of LARU using an intentionally weak LightGBM predictor trained on a single feature and forced to use only one tree during inference, resulting in extremely low prediction accuracy. As shown in Figure 10, FPB suffers severe performance degradation under such inaccurate predictions, with average SLS latency rising sharply. This is observed especially at larger batch sizes. In contrast, LARU remains stable across all cache ratios, batch sizes, and workloads: its latency closely follows that of LRU. This confirms that the robustness mechanism in LARU preserves performance and ensures system stability when integrated with LCR, even in the presence of large prediction errors.

5 Evaluation in LLM Scenarios

5.1 Implementation

We integrate LCR into SGLang 0.4.9 by modifying its default RadixTree cache policy. In this design, RadixTree indices are maintained in DRAM, where prompt prefixes are stored as nodes and their corresponding tensors are placed in GPU HBM. For our experiments, we use GPU HBM exclusively without constructing a hierarchical cache that incorporates DRAM. The original runtime manages evictions using an LRU policy. LCR replaces it with LARU and deploys a LightGBM predictor trained online. Since LARU inherits the structural property of always evicting leaf nodes, it remains fully consistent with SGLang’s RadixTree design, ensuring that shared prefixes are preserved until their descendants are removed.

Given the inherent low concurrency of LLM scenarios compared to DLRMS, we implement LCR in synchronous mode. Workflow type 2 in Figure 7 illustrates the asynchronous workflow of LCR. Due to model complexity, LLMs typically run in low QPS (queries per second) and concurrency, e.g., 10 requests per second and 10 concurrency, whose first token

latency is typically several seconds, making the prediction latency of LightGBM negligible.

LARU and baselines settings. For LARU, the update of λ is implemented as follows: once Line 14 in Algorithm 1 has been executed $k/32$ times, λ is halved, i.e., $\lambda \leftarrow \lambda/2$, where k denotes the cache size. This design avoids overly sensitivity to prediction errors, since k in these scenarios can be large, unlike the slabset size in SlabHash, which is typically 64. For example, if we simply set $b = 2$ when k is large (e.g., 10^3), LARU would converge to LRU after only 10 executions of Line 14 in Algorithm 1, making it difficult to exploit accurate predictions to improve performance.

Similar to the DLRM scenarios (see Section 4), the LLM cases employ LRU and FPB as baselines. In addition, we include HF as a baseline in our robustness evaluation. LRU represents the algorithm used in current LLM inference frameworks, while the latter two represent algorithms adopted in many existing learning-based caching systems.

Predictor settings. Because LLMs run at lower concurrency, with TTFT typically lasting several seconds, which makes the latency of LightGBM negligible, LightGBM is queried and executed in *synchronous mode* in SGLang for all learning-based algorithms. Workflow type 1 in Figure 7 depicts the workflow for this setup. For each eviction function invocation, LightGBM predicts the next-request times of all items in the eviction candidate. The batch prediction task typically costs less than 10 ms in this scenario, since the number of tree nodes in the cache index (RadixTree) is small (typically fewer than 10^4), due to the limited GPU HBM capacity. Note that a tree node typically contains hundreds or even thousands of items due to the aggregation mechanism of the RadixTree. In this setting, LightGBM leverages richer features to improve prediction accuracy. These include the ten most recent request intervals (deltas), ten exponentially decayed counters (EDCs), and the number of tokens along the path from the current tree node to the root, which captures the item’s position within the entire prompt. All items residing in

the same tree node share these features.

Model and hardware settings. We conduct end-to-end experiments on Qwen2.5-32B [36] and Deepseek-R1-671B [10], covering both small and large open-source models. Specifically, we use the 4-bit AWQ-quantized version of Qwen2.5-32B. For Qwen2.5-32B, we use a bare-metal server equipped with four NVIDIA RTX 4090 GPUs and 1TB of DDR5 DRAM. For DeepSeek-R1-671B, we use a bare-metal server with eight NVIDIA H800 GPUs and over 1TB of DDR5 DRAM. Each GPU provides more than 1TB/s of HBM bandwidth, whereas host DRAM reaches only about 120GB/s for random reads.

5.2 Datasets

We use two conversation datasets: one from Company A’s internal QA platform and another synthetically generated with Aibrix [37], an open-source dataset generator developed by the vLLM team. Aibrix provides reproducible, large-scale synthetic workloads for benchmarking LLM systems, with configurable parameters such as request arrivals, input/output lengths, and concurrency.

1. **Online-QA:** A real-world dataset from Company A’s QA platform, containing 2000 conversations and 7268 requests (3.63 per conversation on average) with an average prompt length of 3455 tokens. Because LLM outputs may differ from those in the dataset, evaluation uses only the conversation prompts. Each prompt already includes all preceding turns as a prefix, so model outputs during evaluation are ignored, and the output length is fixed at 256 tokens. Request intervals, defined as the number of intervening requests from other conversations between two consecutive requests, are modeled with a lognormal distribution (mean 266, standard deviation 77.5), consistent with the Qwen-Bailian dataset [39].
2. **Aibrix-Synthetic:** A synthetic dataset generated by the public Aibrix benchmark [37], comprising 500 conversations and 1817 requests (3.63 per conversation on average) with a mean prompt length of 2761 tokens. In Aibrix, both prompts and model outputs from preceding turns are appended as a prefix during evaluation. After the model completes a response, the subsequent request in the conversation is triggered.

5.3 Experimental results

The key to guaranteeing user experience and meeting SLAs in LLM services is reducing TTFT (time to first token), particularly tail latency, which is largely determined by the efficiency of the prefill phase during inference. Accordingly, we report

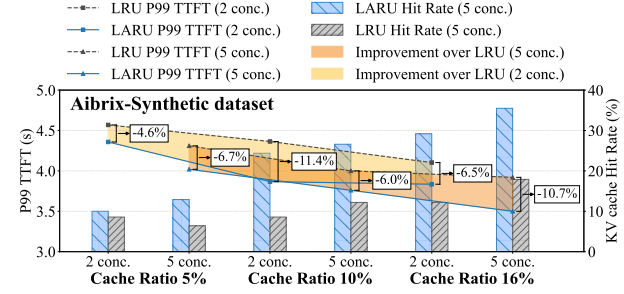


Figure 11: P99 TTFT improvement of Qwen2.5-32B on the Aibrix-Synthetic dataset, where *conc.* denotes concurrency.

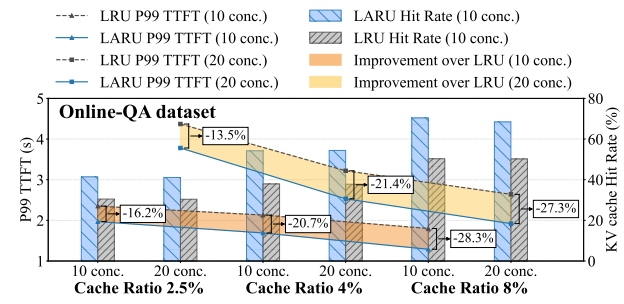


Figure 12: P99 TTFT improvement of DeepSeek-R1-671B on the Online-QA dataset, where *conc.* denotes concurrency.

P99 TTFT as our primary metric, noting that average TTFT exhibits similar reductions and is omitted in this paper.

Across both LLM and DLRM workloads, LARU consistently improves P99 TTFT and cache hit rates over LRU. On the Aibrix-Synthetic dataset with Qwen2.5-32B (Figure 11), LARU reduces P99 TTFT by 6.0%–10.7% at cache ratios between 5% and 16%. On the Online-QA dataset with DeepSeek-R1-671B (Figure 12), LARU achieves even larger gains under higher load: at cache ratios from 2.5% to 8%, P99 TTFT improves by 13.5%–28.3%, with consistent hit-rate increases across both 10- and 20-concurrency settings. These results show that LARU not only reduces tail latency but also maintains its advantage across cache sizes and concurrency levels. Different cache ratios are used for the two datasets due to their differing sizes and the limited capacity of the GPU HBM.

Robustness Verification. Since KV cache hit rate directly translates into reductions in TTFT, we evaluate robustness by injecting controlled noise into the predictor. Specifically, we replace the prediction with the negative of the true next-request time under a given error probability and then measure the resulting hit rates on the Online-QA dataset. When the error probability is 1.0, the predictions are fully inverted from the offline optimal, creating the worst-case scenario. Figure 13 shows that FPB, which follows predictions blindly, collapses rapidly as error probability increases, with hit rates dropping near zero even at modest noise levels. While HF performs

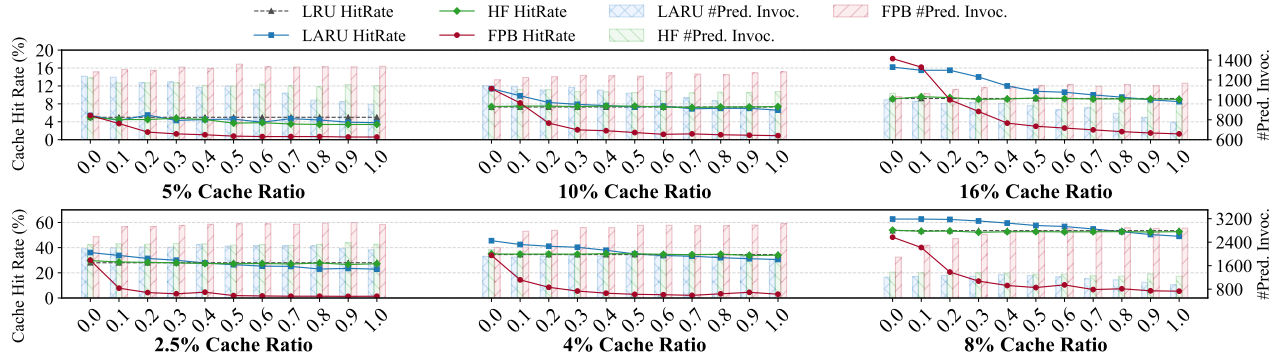


Figure 13: **Robustness Verification.** KV cache hit rate under injected noise on Aibrix-Synthetic (top) and Online-QA (bottom). The probability of replacing predictions with worst-case noise is varied from 0.1 to 1.0.

overly conservatively, without fully benefiting from accurate predictions. In contrast, LARU degrades gracefully, consistently maintaining higher hit rates than both FPB and LRU across all error levels. These results highlight that LARU provides strong robustness: it effectively exploits accurate predictions when available while avoiding catastrophic failure under corrupted predictions. In addition, both LARU and HF make fewer predictor invocations than FPB, with LARU having the lowest usage.

6 Related Work

GPU caching systems. Caching and memory optimization are central to improving the efficiency of large-scale recommendation and language model inference. HugeCTR [42] pioneered GPU-side embedding caches with hierarchical storage, achieving significant throughput gains for DLRMs. Fleche [43] and UGache [33] extend this line of work by designing efficient GPU-resident or multi-GPU caching architectures. These systems demonstrate the importance of GPU caching but rely on static heuristics such as LRU, which fall short under dynamic and diverse workloads.

Learning-based cache algorithms. A large body of work explores using machine learning to guide eviction decisions. HAWKEYE [12] leverages predictive classification to approximate Belady’s optimal policy, while LRB [34] applies gradient boosting for CDN caching. PARROT [22] and GLIDER [32] adopt deep learning models such as LSTMs and imitation learning to mimic the optimal policy. Other approaches, including Raven [11], CACHEUS [29], and LeCaR [38], apply probabilistic modeling, adaptive switching, or online learning to improve eviction. Despite promising results, these methods often *trust predictions blindly*, making them vulnerable to accuracy degradation.

Hybrid and robust designs. To address unreliability, hybrid methods combine heuristics with learned guidance. For

example, HALP [35] and MAT [45] preselect eviction candidates using LRU before applying predictors, which mitigates risk empirically. However, this conservative design in fact fails to provide bounded robustness guarantees and limits the ability to fully leverage accurate predictions. In parallel, the algorithms-with-predictions [24] literature introduces formal robustness guarantees. BLINDORACLE&LRU [41], and PREDICTIVEMARKER [23] balance consistency and robustness, while F&R [31] attains near-optimal guarantees at the cost of prohibitive complexity. These works highlight the fundamental trade-offs among consistency, robustness, and efficiency.

7 Conclusion

We presented LCR, a unified framework for learning-based GPU caching that bridges theoretical robustness guarantees with practical deployability. At its core lies LARU, a new caching algorithm that augments LRU with machine-learned reuse predictions while ensuring ideal 1-consistency, bounded $O(k)$ -robustness, and low $O(\log k)$ per-request complexity. This guarantees LARU’s performance bounds regardless of predictor accuracy. Integrated into both HugeCTR for DLRMs and SGLang for LLMs, LCR demonstrates generality across heterogeneous inference workloads.

Extensive experiments confirm that LCR consistently outperforms classical baselines: on DLRMs, it reduces average SLS latency by up to 19.5%, and on LLM workloads, it lowers P99 TTFT by as much as 28.3%, all while maintaining stable performance under inaccurate predictors. These results highlight the framework’s ability to both exploit accurate forecasts and degrade gracefully when predictions fail.

Looking ahead, LCR lays the groundwork for applying robust learning-based algorithms to GPU memory management. Its design principles extend naturally to broader scenarios, such as GNN training and approximate nearest-neighbor search, opening opportunities for future work on theoretically grounded and deployment-ready caching systems across a

wider range of scenarios.

References

- [1] Sharegpt raw. URL https://huggingface.co/datasets/philschmid/sharegpt-raw/tree/main/sharegpt_90k_raw_dataset.
- [2] The 2nd cache replacement championship, 2017. URL <https://crc2.ece.tamu.edu/>.
- [3] Saman Ashkiani, Martin Farach-Colton, and John D Owens. A dynamic hash table for the gpu. In *2018 IEEE international parallel and distributed processing symposium (IPDPS)*, pages 419–429. IEEE, 2018.
- [4] Nathan Beckmann, Haoxian Chen, and Asaf Cidon. {LHD}: Improving cache hit rate by maximizing hit density. In *15th USENIX Symposium on Networked Systems Design and Implementation (NSDI 18)*, pages 389–403, 2018.
- [5] Allan Borodin and Ran El-Yaniv. Online computation and competitive analysis, 1998.
- [6] Sitian Chen, Haobin Tan, Amelie Chi Zhou, Yusen Li, and Pavan Balaji. Updlrm: Accelerating personalized recommendation using real-world pim architecture. In *Proceedings of the 61st ACM/IEEE Design Automation Conference*, pages 1–6, 2024.
- [7] Feng Cheng, Cong Guo, Chiyue Wei, Junyao Zhang, Changchun Zhou, Edward Hanson, Jiaqi Zhang, Xiaoxiao Liu, Hai Li, and Yiran Chen. Ecco: Improving memory bandwidth and capacity for llms via entropy-aware cache compression. In *Proceedings of the 52nd Annual International Symposium on Computer Architecture*, pages 793–807, 2025.
- [8] Assaf Eisenman, Maxim Naumov, Darryl Gardner, Misha Smelyanskiy, Sergey Pupyrev, Kim Hazelwood, Asaf Cidon, and Sachin Katti. Bandana: Using non-volatile memory for storing deep learning models. *Proceedings of machine learning and systems*, 1:40–52, 2019.
- [9] Amos Fiat, Richard M Karp, Michael Luby, Lyle A McGeoch, Daniel D Sleator, and Neal E Young. Competitive paging algorithms. *Journal of Algorithms*, 12(4):685–699, 1991.
- [10] Daya Guo, Dejian Yang, Haowei Zhang, Junxiao Song, Ruoyu Zhang, Runxin Xu, Qihao Zhu, Shirong Ma, Peiyi Wang, Xiao Bi, et al. Deepseek-r1: Incentivizing reasoning capability in llms via reinforcement learning. *arXiv preprint arXiv:2501.12948*, 2025.
- [11] Xinyue Hu, Eman Ramadan, Wei Ye, Feng Tian, and Zhi-Li Zhang. Raven: belady-guided, predictive (deep) learning for in-memory and content caching. In *Proceedings of the 18th International Conference on emerging Networking EXperiments and Technologies*, pages 72–90, 2022.
- [12] Akanksha Jain and Calvin Lin. Back to the future: Leveraging belady’s algorithm for improved cache replacement. *ACM SIGARCH Computer Architecture News*, 44(3):78–89, 2016.
- [13] Wenqi Jiang, Zhenhao He, Shuai Zhang, Thomas B Preußen, Kai Zeng, Liang Feng, Jiansong Zhang, Tongxuan Liu, Yong Li, Jingren Zhou, et al. Microrec: Efficient recommendation inference by hardware and data structure solutions. *Proceedings of Machine Learning and Systems*, 3:845–859, 2021.
- [14] Wenqi Jiang, Zhenhao He, Shuai Zhang, Kai Zeng, Liang Feng, Jiansong Zhang, Tongxuan Liu, Yong Li, Jingren Zhou, Ce Zhang, et al. Fleetrec: Large-scale recommendation inference on hybrid gpu-fpga clusters. In *Proceedings of the 27th ACM SIGKDD Conference on Knowledge Discovery & Data Mining*, pages 3097–3105, 2021.
- [15] Guolin Ke, Qi Meng, Thomas Finley, Taifeng Wang, Wei Chen, Weidong Ma, Qiwei Ye, and Tie-Yan Liu. Lightgbm: A highly efficient gradient boosting decision tree. *Advances in neural information processing systems*, 30, 2017.
- [16] Liu Ke, Udit Gupta, Benjamin Youngjae Cho, David Brooks, Vikas Chandra, Utku Diril, Amin Firoozshahian, Kim Hazelwood, Bill Jia, Hsien-Hsin S Lee, et al. Rec-nmp: Accelerating personalized recommendation with near-memory processing. In *2020 ACM/IEEE 47th Annual International Symposium on Computer Architecture (ISCA)*, pages 790–803. IEEE, 2020.
- [17] Daniar H Kurniawan, Ruipu Wang, Kahfi S Zulkifli, Fandi A Wiranata, John Bent, Ymir Vigfusson, and Haryadi S Gunawi. Evstore: Storage and caching capabilities for scaling embedding tables in deep recommendation systems. In *Proceedings of the 28th ACM International Conference on Architectural Support for Programming Languages and Operating Systems, Volume 2*, pages 281–294, 2023.
- [18] Woosuk Kwon, Zhuohan Li, Siyuan Zhuang, Ying Sheng, Lianmin Zheng, Cody Hao Yu, Joseph Gonzalez, Hao Zhang, and Ion Stoica. Efficient memory management for large language model serving with page-dattention. In *Proceedings of the 29th Symposium on Operating Systems Principles*, pages 611–626, 2023.

[19] Youngeun Kwon, Yunjae Lee, and Minsoo Rhu. Tensor-dimm: A practical near-memory processing architecture for embeddings and tensor operations in deep learning. In *Proceedings of the 52nd Annual IEEE/ACM International Symposium on Microarchitecture*, pages 740–753, 2019.

[20] Wonbeom Lee, Jungi Lee, Junghwan Seo, and Jaewoong Sim. {InfiniGen}: Efficient generative inference of large language models with dynamic {KV} cache management. In *18th USENIX Symposium on Operating Systems Design and Implementation (OSDI 24)*, pages 155–172, 2024.

[21] Yejin Lee, Seong Hoon Seo, Hyunji Choi, Hyoung Uk Sul, Soosung Kim, Jae W Lee, and Tae Jun Ham. Merci: efficient embedding reduction on commodity hardware via sub-query memoization. In *Proceedings of the 26th ACM International Conference on Architectural Support for Programming Languages and Operating Systems*, pages 302–313, 2021.

[22] Evan Liu, Milad Hashemi, Kevin Swersky, Parthasarathy Ranganathan, and Junwhan Ahn. An imitation learning approach for cache replacement. In *International Conference on Machine Learning*, pages 6237–6247. PMLR, 2020.

[23] Thodoris Lykouris and Sergei Vassilvitskii. Competitive caching with machine learned advice. In Jennifer Dy and Andreas Krause, editors, *Proceedings of the 35th International Conference on Machine Learning*, volume 80 of *Proceedings of Machine Learning Research*, pages 3296–3305. PMLR, 10–15 Jul 2018. URL <https://proceedings.mlr.press/v80/lykouris18a.html>.

[24] Michael Mitzenmacher and Sergei Vassilvitskii. Algorithms with predictions. *Commun. ACM*, 65(7):33–35, June 2022. ISSN 0001-0782. doi: 10.1145/3528087. URL <https://doi.org/10.1145/3528087>.

[25] Michael Mitzenmacher and Sergei Vassilvitskii. Algorithms with predictions. *Communications of the ACM*, 65(7):33–35, 2022.

[26] Yudi Qiu, Lingfei Lu, Shiyan Yi, Minge Jing, Xiaoyang Zeng, Yang Kong, and Yibo Fan. Flips: A flexible partitioning strategy near memory processing architecture for recommendation system. *IEEE Transactions on Parallel and Distributed Systems*, 2025.

[27] Pol G. Recasens, Ferran Agullo, Yue Zhu, Chen Wang, Eun Kyung Lee, Olivier Tardieu, Jordi Torres, and Josep Ll. Berral. Mind the memory gap: Unveiling gpu bottlenecks in large-batch llm inference, 2025. URL <https://arxiv.org/abs/2503.08311>.

[28] Jie Ren, Bin Ma, Shuangyan Yang, Benjamin Francis, Ehsan K Ardestani, Min Si, and Dong Li. Machine learning-guided memory optimization for dlrn inference on tiered memory. In *2025 IEEE International Symposium on High Performance Computer Architecture (HPCA)*, pages 1631–1647. IEEE, 2025.

[29] Liana V Rodriguez, Farzana Yusuf, Steven Lyons, Eysler Paz, Raju Rangaswami, Jason Liu, Ming Zhao, and Giri Narasimhan. Learning cache replacement with {CACHEUS}. In *19th USENIX Conference on File and Storage Technologies (FAST 21)*, pages 341–354, 2021.

[30] Dhruv Rohatgi. Near-optimal bounds for online caching with machine learned advice. In *Proceedings of the Fourteenth Annual ACM-SIAM Symposium on Discrete Algorithms*, pages 1834–1845. SIAM, 2020.

[31] Karim Ahmed Abdel Sadek and Marek Elias. Algorithms for caching and MTS with reduced number of predictions. In *The Twelfth International Conference on Learning Representations*, 2024. URL <https://openreview.net/forum?id=QuIiLSkt04>.

[32] Zhan Shi, Xiangru Huang, Akanksha Jain, and Calvin Lin. Applying deep learning to the cache replacement problem. In *Proceedings of the 52nd Annual IEEE/ACM International Symposium on Microarchitecture*, pages 413–425, 2019.

[33] Xiaoniu Song, Yiwen Zhang, Rong Chen, and Haibo Chen. Ugache: A unified gpu cache for embedding-based deep learning. In *Proceedings of the 29th Symposium on Operating Systems Principles*, pages 627–641, 2023.

[34] Zhenyu Song, Daniel S Berger, Kai Li, Anees Shaikh, Wyatt Lloyd, Soudeh Ghorbani, Changhoon Kim, Aditya Akella, Arvind Krishnamurthy, Emmett Witchel, et al. Learning relaxed belady for content distribution network caching. In *17th USENIX Symposium on Networked Systems Design and Implementation (NSDI 20)*, pages 529–544, 2020.

[35] Zhenyu Song, Kevin Chen, Nikhil Sarda, Deniz Altnbüken, Eugene Brevdo, Jimmy Coleman, Xiao Ju, Paweł Jurczyk, Richard Schooler, and Ramki Gummadi. {HALP}: Heuristic aided learned preference eviction policy for {YouTube} content delivery network. In *20th USENIX Symposium on Networked Systems Design and Implementation (NSDI 23)*, pages 1149–1163, 2023.

[36] Qwen Team. Qwen2 technical report. *arXiv preprint arXiv:2407.10671*, 2024.

[37] The AIBrix Team, Jiaxin Shan, Varun Gupta, Le Xu, Haiyang Shi, Jingyuan Zhang, Ning Wang, Linhui Xu,

Rong Kang, Tongping Liu, et al. Aibrix: Towards scalable, cost-effective large language model inference infrastructure. *arXiv preprint arXiv:2504.03648*, 2025.

[38] Giuseppe Vietri, Liana V Rodriguez, Wendy A Martinez, Steven Lyons, Jason Liu, Raju Rangaswami, Ming Zhao, and Giri Narasimhan. Driving cache replacement with {ML-based}\{LeCaR\}. In *10th USENIX Workshop on Hot Topics in Storage and File Systems (HotStorage 18)*, 2018.

[39] Jiahao Wang, Jinbo Han, Xingda Wei, Sijie Shen, Dingyan Zhang, Chenguang Fang, Rong Chen, Wenyuan Yu, and Haibo Chen. Kvcache cache in the wild: Characterizing and optimizing kvcache cache at a large cloud provider. In *2025 USENIX Annual Technical Conference (USENIX ATC 25)*. USENIX Association, July 2025. URL <https://www.usenix.org/conference/atc25/presentation/wang-jiahao>.

[40] Zehuan Wang, Yingcan Wei, Minseok Lee, Matthias Langer, Fan Yu, Jie Liu, Shijie Liu, Daniel G. Abel, Xu Guo, Jianbing Dong, Ji Shi, and Kunlun Li. Merlin hugectr: Gpu-accelerated recommender system training and inference. In *Proceedings of the 16th ACM Conference on Recommender Systems*, RecSys '22, page 534–537, New York, NY, USA, 2022. Association for Computing Machinery. ISBN 9781450392785. doi: 10.1145/3523227.3547405. URL <https://doi.org/10.1145/3523227.3547405>.

[41] Alexander Wei. Better and simpler learning-augmented online caching. *arXiv preprint arXiv:2005.13716*, 2020.

[42] Yingcan Wei, Matthias Langer, Fan Yu, Minseok Lee, Jie Liu, Ji Shi, and Zehuan Wang. A gpu-specialized inference parameter server for large-scale deep recommendation models. In *Proceedings of the 16th ACM Conference on Recommender Systems*, pages 408–419, 2022.

[43] Minhui Xie, Youyou Lu, Jiazen Lin, Qing Wang, Jian Gao, Kai Ren, and Jiwu Shu. Fleche: an efficient gpu embedding cache for personalized recommendations. In *Proceedings of the Seventeenth European Conference on Computer Systems*, pages 402–416, 2022.

[44] Gang Yan, Jian Li, and Don Towsley. Learning from optimal caching for content delivery. In *Proceedings of the 17th International Conference on emerging Networking EXperiments and Technologies*, pages 344–358, 2021.

[45] Dongsheng Yang, Daniel S Berger, Kai Li, and Wyatt Lloyd. A learned cache eviction framework with minimal overhead. *arXiv preprint arXiv:2301.11886*, 2023.

[46] Juncheng Yang, Ziming Mao, Yao Yue, and KV Rashmi. {GL-Cache}: Group-level learning for efficient and high-performance caching. In *21st USENIX Conference on File and Storage Technologies (FAST 23)*, pages 115–134, 2023.

[47] Lingyun Yang, Yongchen Wang, Yinghao Yu, Qizhen Weng, Jianbo Dong, Kan Liu, Chi Zhang, Yanyi Zi, Hao Li, Zechao Zhang, et al. {GPU-Disaggregated} serving for deep learning recommendation models at scale. In *22nd USENIX Symposium on Networked Systems Design and Implementation (NSDI 25)*, pages 847–863, 2025.

[48] Guanghu Yuan, Fajie Yuan, Yudong Li, Beibei Kong, Shujie Li, Lei Chen, Min Yang, Chenyun Yu, Bo Hu, Zang Li, et al. Tenrec: A large-scale multipurpose benchmark dataset for recommender systems. *Advances in Neural Information Processing Systems*, 35:11480–11493, 2022.

[49] Yazhuo Zhang, Juncheng Yang, Yao Yue, Ymir Vigfusson, and KV Rashmi. {SIEVE} is simpler than {LRU}: an efficient {Turn-Key} eviction algorithm for web caches. In *21st USENIX Symposium on Networked Systems Design and Implementation (NSDI 24)*, pages 1229–1246, 2024.

[50] Zhe Zhang, Ziyue Luo, and Chuan Wu. Two-level graph caching for expediting distributed gnn training. In *IEEE INFOCOM 2023-IEEE Conference on Computer Communications*, pages 1–10. IEEE, 2023.

[51] Weijie Zhao, Shulong Tan, and Ping Li. Song: Approximate nearest neighbor search on gpu. In *2020 IEEE 36th International Conference on Data Engineering (ICDE)*, pages 1033–1044. IEEE, 2020.

[52] Lianmin Zheng, Liangsheng Yin, Zhiqiang Xie, Chuyue Livia Sun, Jeff Huang, Cody Hao Yu, Shiyi Cao, Christos Kozyrakis, Ion Stoica, Joseph E Gonzalez, et al. Sqlang: Efficient execution of structured language model programs. *Advances in Neural Information Processing Systems*, 37:62557–62583, 2024.

[53] Guorui Zhou, Na Mou, Ying Fan, Qi Pi, Weijie Bian, Chang Zhou, Xiaoqiang Zhu, and Kun Gai. Deep interest evolution network for click-through rate prediction. In *Proceedings of the AAAI conference on artificial intelligence*, volume 33, pages 5941–5948, 2019.

[54] Wenbin Zhou, Zhixiong Niu, Yongqiang Xiong, Juan Fang, and Qian Wang. {3L-Cache}: Low overhead and precise learning-based eviction policy for caches. In *23rd USENIX Conference on File and Storage Technologies (FAST 25)*, pages 237–254, 2025.

Artifact Appendix

Abstract

The provided artifacts include all code and non-confidential traces to reproduce the experimental results presented in the paper. They integrate LCR into two open-source inference frameworks, one for DLRMs and the other for LLMs.

Scope

These artifacts are capable of verifying both the improved performance and robustness guarantees of LCR in GPU caching with fixed-size items, including embedding vector caching in DLRMs and KV caching in LLMs.

1. **SLS-Cache-Bench.** For DLRMs, we develop a dedicated benchmark that isolates the SparseLengthsSum (SLS) operation from the HugeCTR framework and integrates LCR. The benchmark supports direct comparison of GPU embedding cache policies, including FPB (following predictions blindly), LARU, and classical LRU. We implement an alternative GPU cache in the `flash_cache` directory while retaining the original cache indices and `SlabHash`, and enable host-to-device transfer of predictions to realize the logic of LARU. The implementation comprises roughly 25K lines of code, including 16K C/C++ and 3.5K CUDA, together with build and configuration scripts. These modifications make the benchmark self-contained, reproducible, and extensible for future evaluation.

This artifact enables reproduction of results on the public QB-video dataset presented in Section 4.3 (Figures 7 and 8). In addition, the cache hit rate gap between LRU and the offline optimal (OPT) on the QB-video dataset (Figure 4) can be measured using the provided script.

2. **LCR-on-SGLang.** For LLMs, we integrate LCR into SGLang (version 0.4.9.post2) by adding LightGBM support, implementing an online training framework, and replacing the default RadixTree cache (`radix_cache.py`) with LARU. This integration enables systematic comparison of GPU KV cache policies, including FPB, LARU, and classical LRU. It comprises over 5K lines of new code, including a new RadixTree cache implementation (`laru_radix_cache.py`) and predictor modules, excluding LightGBM checkpoints and configuration files. These extensions provide a robust basis for a comprehensive evaluation of LCR under LLM inference workloads.

This artifact enables reproduction of results on the Aibrix-Synthetic dataset presented in Section 5.3 (Figures 9 and 11). In addition, the cache hit rate gap between LRU and the offline optimal (OPT) on the Aibrix-

Synthetic dataset (Figure 4) can be measured using the provided script.

Contents

We have outlined the core modifications of the artifacts in the **Scope** section above. Detailed usage instructions are available in the `README.md` file.

Requirements

The artifact has distinct software requirements for the DLRM and LLM scenarios:

1. DLRMs: CUDA 12.4, PyTorch 2.6.0, and either `devtoolset-9` or `gcc-9`.
2. LLMs: CUDA 12.6, PyTorch 2.6.0, and the required third-party Python packages, `lightgbm`.

The hardware used to generate the results in this paper is described in Section 4.1 for DLRMs and Section 5.1 for LLMs. Nevertheless, the experiments can also be conducted on other GPUs, provided that the available HBM capacity is sufficient to accommodate both the ML models and the GPU cache.

Technical Appendix

A Performance Metrics

The performance of an online caching algorithm ALG is measured by its *competitive ratio*, defined as

$$\alpha(\text{ALG}) := \sup_I \frac{\text{ALG}(I)}{\text{OPT}(I)},$$

where I is an input sequence, and $\text{ALG}(I)$ and $\text{OPT}(I)$ denote the costs incurred by ALG and the offline optimal algorithm OPT, respectively. We say that ALG is $\alpha(\text{ALG})$ -competitive. In the online caching problem with uniform item sizes (paging), the cost is the number of cache misses.

For learning-based caching, the *consistency* of ALG is its competitive ratio under perfectly accurate predictions, while its *robustness* is its competitive ratio under completely inaccurate predictions.

B Key Observation

Let OPT be the offline optimal algorithm following Belady’s rule. It never keeps an item in the cache that is not requested during the interval between the eviction and the next request of another item.

Proof. Suppose a request for item x at time t incurs a miss, and x was evicted by OPT at some earlier time t' ($t' < t$). If some item y remains in the cache at time t without being requested during (t', t) , then at time t' the next request of y must occur strictly later than that of x . By Belady’s rule, OPT would have evicted y instead of x , yielding a contradiction. \square

C LARU’s Theoretical Properties

With cache size k , LARU provides the following guarantees:

- Bounded robustness.** The robustness of LARU is $O(k)$, as proved in Technical Appendix D. In other words, regardless of predictor accuracy, its competitive ratio is bounded by $O(k)$, matching LRU’s k -competitive ratio asymptotically and safeguarding against catastrophic performance degradation or systemic risk.
- Ideal consistency.** The consistency of LARU is 1, as proved in Technical Appendix E. Under perfect predictions, LARU matches the offline optimal algorithm, fully leveraging accurate machine-learned predictions.
- Low time complexity.** The algorithm runs in $O(\log k)$ amortized time per request, which is practical since k is small in practice. In DLRMs, embedding caches are partitioned into buckets (e.g., SlabHash in HugeCTR),

each holding only tens of items (e.g., 64). In LLMs, KV cache vectors are typically organized via RadixTrees in SGLang or paged-attention in vLLM, with total cached items typically not exceeding 10^4 .

- Reduced predictor usage.** In asynchronous mode, prediction tasks are triggered only under specific conditions, such as at most once per fixed interval or after the previous task has completed, preventing excessive usage. In synchronous mode, once a prediction-induced cache miss is detected (Line 14 in Algorithm 1), LARU falls back to LRU once, limiting predictor calls and reducing the candidate set in the next prediction-driven eviction (Line 25), which lowers predictor overhead. We evaluate the number of predictor invocations in Section 5.3, specifically for LLM scenarios operating under synchronous mode.

D Proof of LARU’s $O(k)$ -Robustness

Before analyzing the robustness of LARU, we first establish the cost bound of OPT in Lemma 1.

Suppose the N -th phase is the last completed phase after n requests have been served. Let c_i denote the number of distinct new items requested in the i -th phase. Lemma 1 then establishes the cost bounds of OPT.

Lemma 1. $\text{OPT}(I) \geq \max\left(\frac{1}{2} \sum_{i=1}^N c_i, N - 1\right)$.

Proof. First, we show that $\text{OPT} \geq N - 1$. Split the request sequence into intervals from the beginning, and close each interval once it contains k distinct items, with the next request going to a new item that is not among these k distinct items. Let p_j^i denote the j -th distinct item in interval i . OPT must incur at least one miss when serving p_2^i, \dots, p_k^i and p_1^{i+1} , since p_1^i is already in the cache. Thus, for a sequence with X intervals, OPT incurs at least $X - 1$ misses. Moreover, each phase in LARU contains at least k distinct items, since a phase ends only after every old item has been either requested or evicted. Then, a sequence with N phases can be partitioned into at least N intervals, implying that OPT incurs at least $N - 1$ misses.

Next, we prove that $\text{OPT} \geq \frac{1}{2} \sum_{i=1}^N c_i$. Let c_i denote the number of distinct new items requested in the i -th phase. Define OPT_i as the number of misses incurred by OPT in the i -th phase. Let h_i ($1 \leq i \leq N$) denote the number of pages in OPT’s cache but not in LARU’s cache at the beginning of phase i , noting that $h_1 = 0$ since both caches start empty.

Within the i -th phase, at most h_i of the c_i new requests may already reside in OPT’s cache. Thus,

$$\text{OPT}_i \geq c_i - h_i. \quad (1)$$

At the beginning of phase $(i+1)$, OPT contains h_{i+1} pages not present in LARU, and thus misses h_{i+1} pages that reside

in LARU. Since every page in LARU's cache at the end of phase i must have been requested during that phase, OPT must have evicted at least h_{i+1} pages in phase i :

$$\text{OPT}_i \geq h_{i+1}. \quad (2)$$

If an unfinished $(N+1)$ -th phase exists after n requests, we ignore its contribution, as it vanishes in the asymptotic competitive ratio when $N \rightarrow \infty$.

Combining (1) and (2), we obtain:

$$\begin{aligned} \text{OPT} &= \sum_{i=1}^N \text{OPT}_i \geq \sum_{i=1}^N \max(c_i - h_i, h_{i+1}) \\ &\geq \sum_{i=1}^N \frac{1}{2} (c_i - h_i + h_{i+1}) \\ &\geq \sum_{i=1}^N \frac{1}{2} c_i. \end{aligned} \quad (3)$$

Therefore,

$$\text{OPT} \geq \max\left(\frac{1}{2} \sum_{i=1}^N c_i, N - 1\right), \quad (4)$$

which completes the proof. \square

Theorem 1. *The robustness of LARU is $O(k)$.*

Proof. First, within a phase, there can be at most k evictions following LRU's policy. Since the items in O have not been requested during the current phase, their last request times are always earlier than those of items outside O . Hence, LRU policy must evict items from O within a phase. After k such evictions, O must be empty, and a new phase begins.

Next, we consider evictions based on predictions within phase i , where $1 \leq i \leq N$. LARU performs such evictions in two cases:

1. the requested item is a new item that has not yet been evicted in the current phase.
2. the requested item was previously evicted by LRU's policy within the same phase.

The number of occurrences of case (1) equals the number of distinct new items, c_i . Note that after $\log_b(k)$ occurrences of case (2), λ has become $1/b^{\log_b(k)}$, the candidate set \mathcal{L} shrinks to size 1, and the eviction step at Line 25 degenerates to LRU's policy. Hence, the number of prediction-based evictions with $|\mathcal{L}| > 1$ is at most $c_i + \log_b(k)$.

Additionally, the number of LRU-following evictions at Line 15 and at Line 25 with $|\mathcal{L}| = 1$ is at most k in a phase. Therefore, the total number of evictions of LARU is

$$N(k + \log_b(k)) + \sum_{i=1}^N c_i. \quad (5)$$

According to Lemma 1, we have

$$\lim_{N \rightarrow \infty} \frac{\text{LARU}(\mathbf{I})}{\text{OPT}(\mathbf{I})} \leq k + \log_b(k) + 2. \quad (6)$$

Since $\log_b(k) \leq k$ by definition, (6) establishes the $O(k)$ -robustness of LARU, completing the proof. \square

E Proof of LARU's 1-Consistency

Theorem 2. *The consistency of LARU is 1.*

Proof. With perfectly accurate predictions, LARU evicts at Line 25 the item z whose next request is furthest in the future. Since all other cached items are requested before z reappears, O becomes empty and a new phase begins before z 's next request. Thus, the condition in Line 14 is never satisfied when z is requested again. Consequently, LARU always evicts according to predictions, with $\lambda = 1$ holding throughout, and therefore behaves identically to OPT. \square